Advances in Industrial and Manufacturing Engineering 5 (2022) 100089

Contents lists available at ScienceDirect

Advances in Industrial and Manufacturing Engineering

journal homepage: www.elsevier.com/locate/aime

Regular articles

Introducing engineering undergraduates to CNC machine tool error compensation

Abhijit Bhattacharyya [a,*], Tony L. Schmitz [b], Scott W.T. Payne [c], Palash Roy Choudhury [a], John K. Schueller [d]

[a] Mechanical Engineering, Mahindra University, Hyderabad, India
[b] Mechanical, Aerospace & Biomedical Engineering, University of Tennessee, Knoxville, TN, United States of America
[c] Halliburton Jet Research Center, Alvarado, TX, United States of America
[d] Mechanical & Aerospace Engineering, University of Florida, Gainesville, FL, United States of America

ARTICLE INFO

Keywords:
Machine tool accuracy
Homogeneous transformation matrices
HTM
Geometric accuracy of machine tool
Error compensation

ABSTRACT

For manually operated machine tools, the accuracy of the machine tool structure limits the accuracy of the parts produced. Such is not necessarily the case with computer numerically controlled (CNC) machine tools. This concept may not be immediately obvious to the engineering undergraduate. The method of error compensation is presented here in a manner that is accessible to the undergraduate engineering student. A homogeneous transformation matrix (HTM) model quantifies the geometric errors of a machine tool, which can be compensated for in software. The mathematical treatment is reduced to only essential elements to emphasize physical understanding. A key feature of this presentation is the application of the model to a three-axis milling machine. This illustration enables the undergraduate student to grasp the concept with ease. Another feature is that the entire model is developed from first principles, which does not require the student to invoke any empirical relationships. Three solved numerical problems illustrate the application of the model to practical situations. Information provided here may be used by the teacher as a template to introduce this subject at the undergraduate level.

1. Educational features of this paper

We present the pedagogy for introducing engineering undergraduate students to geometric error compensation for CNC machine tools. In the digital manufacturing ecosystem of today, this represents a foundational capability for students. The presentation offers several unique educational features

(1) All the analysis is based on first principles.
(2) A specific mathematical model for capturing machine tool accuracy is introduced which does not find mention in any undergraduate manufacturing textbook, except for one text (Tlusty, 1999) in which it is indirectly suggested.
(3) Relevant fundamentals required for the understanding of the accuracy assurance model are first introduced in a compact fashion.
(4) The student is stepped through the development of the model in a sequential and logical manner.
(5) In an illustrative example, the model is applied to a three-axis machine tool to demonstrate its application. This is our unique contribution. We are not aware of any publication where the model is applied in such a direct and straightforward manner so that it appeals to the first-time student of the subject.
(6) The instructor can use this paper as a standalone teaching material. All the matter required for a scientific introduction to the subject is presented here, including three solved exercise problems.
(7) The purpose of providing references is to supplement the instructor in teaching. The student is not required to study the references. From the point of view of the student, the matter presented here is complete, and sufficient for undergraduate studies.

2. Background

The subject matter of this document was first introduced into a manufacturing engineering textbook by a pioneer in machine tool design, the late Jiri (George) Tlusty. His text (Tlusty, 1999) remains the only one, among a host of excellent manufacturing texts (Kalpakjian

* Corresponding author.
E-mail address: diroindia@gmail.com (A. Bhattacharyya).

https://doi.org/10.1016/j.aime.2022.100089
Received 25 March 2022; Received in revised form 14 June 2022; Accepted 15 June 2022
Available online 20 June 2022

and Schmid, 2018; Groover, 2013; Ghosh and Mallik, 1992; Black and Kohser, 2019; Schey, 2012), to even mention this topic, which improves student understanding of how accurate parts can be produced by modern CNC machines. In this paper, we offer a variant of the method proposed in his text, to make it more accessible to the senior undergraduate student. Our method explicitly uses the homogeneous transformation matrix (HTM) model, first proposed by Donmez (1985), to which (Tlusty, 1999) has alluded to indirectly. Slocum (1992) provides a comprehensive description of HTMs in his textbook aimed at the graduate student and the professional machine tool designer.

Though this topic does not find mention in most undergraduate manufacturing engineering texts, except (Tlusty, 1999), it has a place in the modern manufacturing curriculum at the undergraduate level, being of utmost importance in manufacturing process equipment design. Here, we present a method which we have successfully used to introduce the subject to senior undergraduate students. The material presented in this paper can be delivered over two or three lectures, in what might typically be a 35 to 40 lecture manufacturing engineering course.

3. Factors influencing machined part dimensional accuracy

Two broad classes of factors affect the dimensional accuracy of machined parts (Donmez, 1985; Donmez et al., 1986; Slocum, 1992; Tlusty, 1999), each of which is composed of different components

(1) Inherent machine inaccuracies due to the construction of the machine tool structure, including structural deflections due to structural weight, resulting in so-called **geometrical inaccuracies** of the machine tool. These are the inaccuracies we address in this paper as we are interested in assessing the accuracy of machine construction, and compensating for these.
(2) Operational inaccuracies, which show up when the machining operation is being performed, due to thermal expansion effects, structural deflections in the tool-workpiece-machine system due to cutting forces, tool wear effects, and clamping accuracy effects. Predictive models and control strategies can be employed to assess and compensate for these inaccuracies, but they are not within the scope of this paper.

4. The sources of machine tool inaccuracy

To manufacture a part accurately, the tool point must be brought into the correct position with respect to the workpiece, i.e., we seek to model this tool positioning error. A workpiece or a tool may be rigidly clamped onto a spindle or carriage, which moves over a slideway/guideway. The sources of geometric inaccuracy are

(1) Inaccuracies in the motion of carriages/spindles over slideways, and
(2) Carriage/spindle position measurement inaccuracies due to measuring scale locations

We distinguish between the above two sources based on the fact that the first one is owing to physical inaccuracies in machine structure construction such as angular errors associated with linear motion, and the second one is due to measuring scale locations.

The first source of inaccuracy is connected with the cost of design and manufacture of highly accurate slideway structures. The accuracy that a machine tool designer would like to build into the machine structure affects the cost of manufacturing the machine, but this cost always needs to be contained within certain specified limits. So, building a super accurate machine tool structure may not be an economically feasible option.

The second source of inaccuracy due to the placement of carriage/spindle position measuring scales is inherent, and it is one that is impossible to eliminate. To understand this, we consider two principles of measurement, namely, the Abbé principle (Abbé, 1890), and the Bryan principle (Bryan, 1979), which are explained in what follows.

The Abbé principle states that (Leach, 2014), "If errors of parallax are to be avoided, the measuring system must be placed co-axially (in line with) the line in which displacement (given length) is to be measured on the work-piece". It is easily illustrated as shown in Figs. 1 and 2. Suppose we measure the diameter of a circular cylinder using a micrometer. The measuring scale sits right in line with the diameter being measured. However, measuring the diameter using a caliper leads to a possible Abbé offset error if the jaws of the caliper do not stay exactly parallel during measurement. Since the measurement scale is offset with respect to the diameter of the part being measured, any lack of parallelism of the jaws results in the angular error being converted into a linear scale error by the Abbé offset.

In machine tools, we usually have compound motions, because several slides move over each other in a serial kinematic chain {Parallel kinematic machines are not a subject of our discussions, although many of the mathematical principles described herein will apply}. For this reason, it becomes impossible to obey Abbé's principle while designing the placement of measuring scales.

5. A strategy for producing accurate parts: compensation in software

The **Bryan principle** is a generalized Abbé principle. To quote (Bryan, 1979), "if it is not possible to obey the Abbé principle, either the slideways that transfer the displacement must be free of angular motion or angular motion data must be used to calculate the consequences of the offset". This last sentence provides a key to how the problem of assuring machining accuracy may be approached. If we are able to calculate the consequences of disobeying Abbé, we will be able to compensate for it. The computerized machine controller could be commanded to implement **compensation in software** based on calculated inaccuracies. The strategy, therefore, is to rely on a mathematical model of the inbuilt inaccuracies in the machine tool. The controller could anticipate the modeled inaccuracies, and compensate in real time as the carriage/spindle moves over the slideway/guideway. As a result, a machine tool which has these inbuilt inaccuracies could be used to manufacture a part of desired dimensional accuracy. Alternatively, a coordinate measuring machine could probe a part with a desired level of accuracy. Such a scheme for the servo control of the motion of a single axis of a machine, in which the position feedback is appropriately modified for error using calculations based on an error model, is shown in Fig. 3.

How can we come up with a mathematical model to tell us where the tool and workpiece are mutually positioned based on what the measurement scales are telling us, even though the scales may not be in line with the motion of the tool and/or the workpiece which are fixed on the spindle and the carriage? This is a rigid body kinematics problem.

The tool-workpiece positioning model developed in this paper is a rigid-workpiece rigid-tool rigid-machine-structure model which is concerned with the geometric accuracy related to carriage/spindle motions and positioning, and forms the starting point in understanding this complex phenomenon of machine tool accuracy.

The general displacement of a rigid body can be described on the basis of the Chasles–Mozzi–Cauchy theorem (Whittaker, 1917; Baruh, 1999) which states that the most general rigid body displacement can be produced by a translation along a line followed, or preceded, by a rotation about that line. In this paper, we decompose the rotation into three components which are individual rotations about the axes of some reference frame attached to the body, with its origin on the axis of rotation, and then translate this origin to obtain the required displacement, or vice versa.

First, we model rotations. Next we present a way of combining the translation with this rotation to obtain the final position and orientation

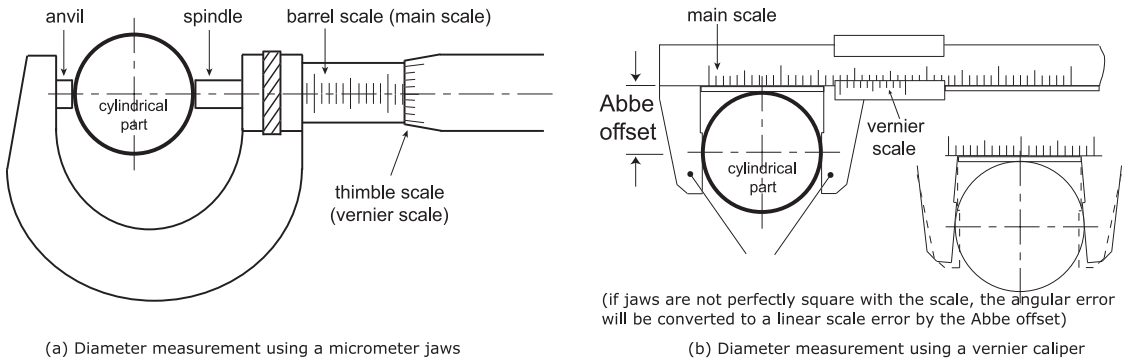

Fig. 1. Illustration of (a) the absence of any Abbé offset error, and (b) the possibility of the Abbé error owing to the offset.

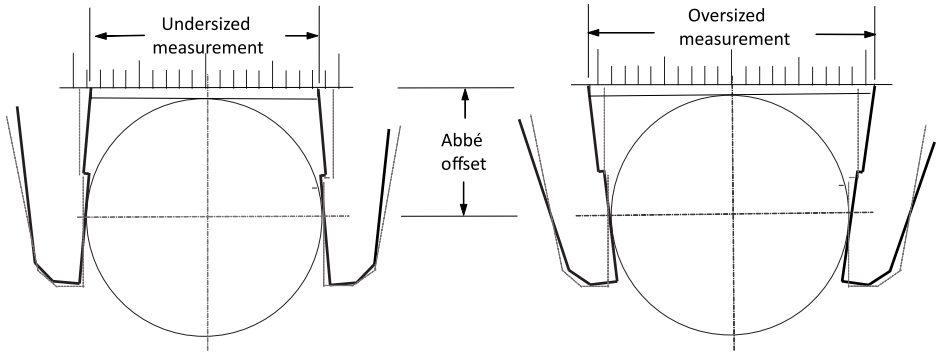

Fig. 2. Possible consequences of the Abbé offset error: (left) underestimation and (right) overestimation of the measured dimension depending on the orientation of the angular error (non-parallelism of measuring instrument faces in this case).

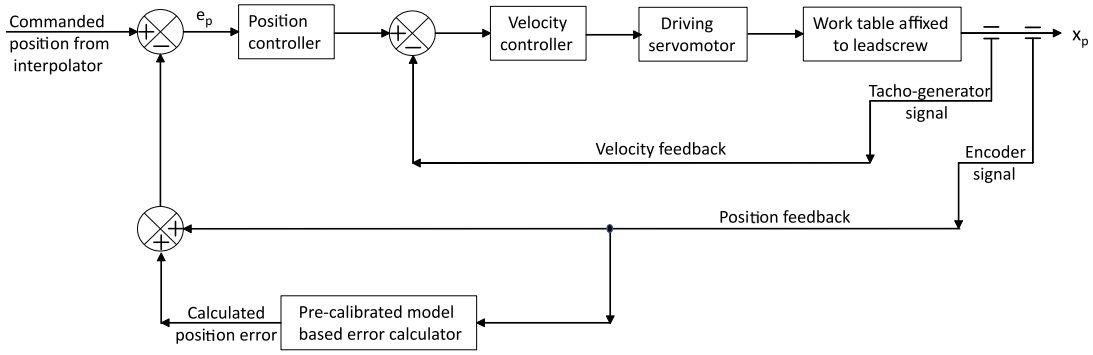

Fig. 3. Work-table position control with compensation in software using model based error calculation.

of the rigid bodies (the tool and the workpiece), whose motions we are studying. Finally, we incorporate errors of motions into the model. Doing so reveals the error in tool positioning with respect to the workpiece, which can be compensated for in the controller software.

6. Mathematical toolkit

The mathematical toolkit which the student requires comprises basic matrix algebra and the ability to interpret column vectors. It suffices if the student can assemble a set of linear equations into a vector–matrix equation form, is able to understand the meaning of the transpose of a matrix, and is able to multiply matrices. Furthermore, it is helpful if the student is able to comprehend the meaning of the inverse of a matrix, though the ability to invert is not required. Sophomore and junior level students are usually equipped to handle such algebra, and senior level undergraduate engineering students would certainly be expected to do so.

7. Modeling rotations

Let us consider a rectilinear Cartesian coordinate system, $\mathfrak{F}_A$, with its origin at O, and a different Cartesian coordinate system, $\mathfrak{F}_B$, placed at the same origin, but oriented differently from the frame, $\mathfrak{F}_A$. Let ${}^A\mathbf{r}_P$ be the position vector of a particle, P, coordinatized in frame $\mathfrak{F}_A$ and ${}^B\mathbf{r}_P$ be its position vector coordinatized in frame $\mathfrak{F}_B$. These two position vectors are related through a rotation matrix (Whittaker, 1917; Baruh, 1999), ${}^A R_B$, such that

$$ {}^A\mathbf{r}_P = {}^A R_B \, {}^B\mathbf{r}_P \tag{1} $$

In expanded form we may write this relationship as follows

$$ \begin{Bmatrix} x_A \\ y_A \\ z_A \end{Bmatrix} = \begin{bmatrix} r_{11} & r_{12} & r_{13} \\ r_{21} & r_{22} & r_{23} \\ r_{31} & r_{32} & r_{33} \end{bmatrix} \begin{Bmatrix} x_B \\ y_B \\ z_B \end{Bmatrix} \tag{2} $$

The 3 × 3 rotation matrix is orthogonal (Hogben, 2007). All the rows and columns are normalized and all inner products are zero. Being

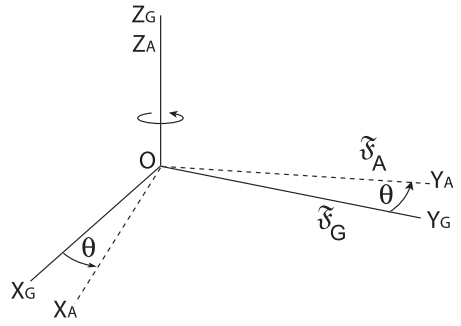

Fig. 4. Local frame rotated by angle θ about z_G to a new orientation $\mathfrak{F}_A$. The rotation matrix is $R(z,\theta)$.

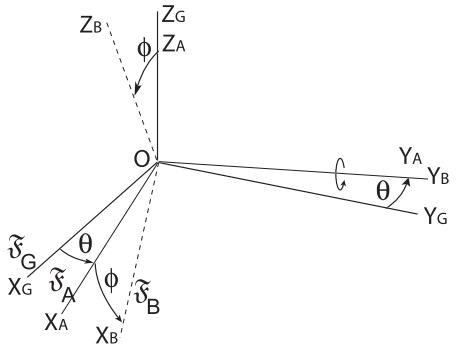

Fig. 5. Local frame $\mathfrak{F}_A$ rotated by angle ϕ about y_A to a new orientation $\mathfrak{F}_B$. The rotation matrix is $R(y,\phi)$.

orthogonal, its transpose equals the inverse (Hogben, 2007), which is convenient for two reasons. First, the inverse always exists, allowing us to go back and forth between the frames. Second, the inverse never needs to be computed. Writing down the transpose suffices.

How do we populate this matrix for a general rotation about a fixed point? It is always possible to find a set of three successive rotations about three mutually perpendicular axes such that any final orientation of a rigid body may be attained, starting from an arbitrary initial orientation {in fact we can get to any orientation by a single rotation about a specific line passing through a fixed point, the Euler axis, which is Euler's fundamental theorem on rigid body rotation (Whittaker, 1917; Baruh, 1999), but our aim is to model rotational errors about three mutually perpendicular axes in a machine tool or a coordinate measuring machine}.

Let us consider a fixed global frame $\mathfrak{F}_G$. Let us also consider a rigid body to which we attach a local frame. Let us align this local frame with $\mathfrak{F}_G$ with their origins coinciding. In this configuration, we do not give the local frame a name but understand that it is identically aligned with the global frame. We like to track the motion of a point P fixed in the local frame (i.e., P is a point on the rigid body) as the orientation of the rigid body is changed by an arbitrary rotation about the origin, O (pure rotation). Taking the counterclockwise sense of rotation as positive, let us rotate the local frame (the rigid body) through three successive rotations to reach a different orientation in the following fashion

(1) Rotate the local frame by an angle θ about the z_G axis of $\mathfrak{F}_G$ to obtain a new orientation of the local frame which we call $\mathfrak{F}_A$, as shown in Fig. 4.
(2) Rotate the frame $\mathfrak{F}_A$ by an angle ϕ about the y_A axis of $\mathfrak{F}_A$ to obtain a new orientation of the frame which we may call $\mathfrak{F}_B$, as shown in Fig. 5. We notice that we rotated about an axis of the current position of the frame, not about any original axis of $\mathfrak{F}_G$. By doing so, we are assured of being able to use the rotation matrices to transform to each successive coordinate system.
(3) Rotate the frame $\mathfrak{F}_B$ by an angle ψ about the x_B axis of $\mathfrak{F}_B$ to obtain a new orientation of the frame which we may call $\mathfrak{F}_C$, as shown in Fig. 6.

We notice that we rotated about different axes z_G, y_A, and x_B. Such a rotation is called a 3-2-1 rotation, corresponding to the $z-y-x$ sequence of axes about which the successive rotations are made. Other possibilities exist, such as 1-2-3 or 3-1-3, etc. Of the 27 such possibilities, there are 12 sets in which consecutive numbers do not repeat, i.e., we do not admit sequences such as 1-1-3. These 12 sets are known as Euler angle sequences (Baruh, 1999). Of these, we may use any of the six sets in which the axes are not repeated, such as 1-2-3 or 3-2-1, etc. We do so for convenience as we will apply these to capture rotational errors about the three mutually orthogonal linear axes in machine tools.

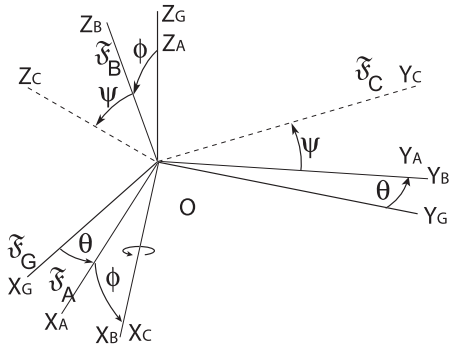

Fig. 6. Local frame $\mathfrak{F}_B$ rotated by angle ψ about x_B to a new orientation $\mathfrak{F}_C$. The rotation matrix is $R(x,\psi)$.

Now, let us consider the position vector of the point P in the frame $\mathfrak{F}_C$. Since the body to which the frame is attached is rigid, we always know ${}^C\mathbf{r}_P$. Do we know ${}^B\mathbf{r}_P$? The rotation matrix provides the link as follows

$$ {}^B\mathbf{r}_P = {}^B R_C \, {}^C\mathbf{r}_P = R(x,\psi)\,{}^C\mathbf{r}_P \tag{3} $$

where the equivalent notation for the rotation matrix, $R(x,\psi)$, is also shown. This second notation is commonly used in analytical dynamics literature (Schuster, 1993).

Similarly

$$ {}^A\mathbf{r}_P = {}^A R_B \, {}^B\mathbf{r}_P = R(y,\phi)\,{}^B\mathbf{r}_P \tag{4} $$

Combining the equations (3) and (4), we have

$$ {}^A\mathbf{r}_P = {}^A R_B \, {}^B R_C \, {}^C\mathbf{r}_P = R(y,\phi)R(x,\psi)\,{}^C\mathbf{r}_P \tag{5} $$

Finally the position vector in the fixed global frame $\mathfrak{F}_G$

$$ \begin{aligned} {}^G\mathbf{r}_P &= {}^G R_A \, {}^A\mathbf{r}_P = {}^G R_A \, {}^A R_B \, {}^B R_C \, {}^C\mathbf{r}_P \\ &= R(z,\theta)R(y,\phi)R(x,\psi)\,{}^C\mathbf{r}_P = R_{321}(\theta,\phi,\psi)\,{}^C\mathbf{r}_P \end{aligned} \tag{6} $$

We observe that we have a product of the rotation matrices, which is convenient for computations. Multiplying the three rotation matrices yields the fully populated rotation matrix of equation (2), which we now denote as $R_{321}(\theta,\phi,\psi)$ $\{= R(z,\theta)R(y,\phi)R(x,\psi)\}$, using the Euler sequence 3-2-1. Individual rotation matrices are easily computed using elementary coordinate transformations. The results (Baruh, 1999;

Whittaker, 1917; Schuster, 1993) are listed below

$$R(z,\theta)=\begin{bmatrix}\cos\theta & -\sin\theta & 0\\ \sin\theta & \cos\theta & 0\\ 0 & 0 & 1\end{bmatrix},\quad R(y,\phi)=\begin{bmatrix}\cos\phi & 0 & \sin\phi\\ 0 & 1 & 0\\ -\sin\phi & 0 & \cos\phi\end{bmatrix},$$
$$R(x,\psi)=\begin{bmatrix}1 & 0 & 0\\ 0 & \cos\psi & -\sin\psi\\ 0 & \sin\psi & \cos\psi\end{bmatrix} \tag{7}$$

Matrix multiplication yields the populated rotation matrix, $R_{321}(\theta,\phi,\psi)$

$$R_{321}(\theta,\phi,\psi)=\begin{bmatrix}\cos\theta\cos\phi & \cos\theta\sin\phi\sin\psi-\sin\theta\cos\psi & \cos\theta\sin\phi\cos\psi+\sin\theta\sin\psi\\ \sin\theta\cos\phi & \sin\theta\sin\phi\sin\psi+\cos\theta\cos\psi & \sin\theta\sin\phi\cos\psi-\cos\theta\sin\psi\\ -\sin\phi & \cos\phi\sin\psi & \cos\phi\cos\psi\end{bmatrix} \tag{8}$$

This matrix corresponds to a 3-2-1 Euler rotation sequence. If we had taken a different sequence of rotations, say 2-1-3, the form of the rotation matrix would have turned out to be different. When finite rotations are considered, the operation of multiplication of rotation matrices is not commutative (Baruh, 1999). The order of rotations is important.

However, for infinitesimal rotations, the operation of multiplication of rotation matrices is commutative (Baruh, 1999). Let us consider small rotations and examine the form of the rotation matrix seen in equation (8). For small angles of rotation, we set the cosines of the rotations equal to unity, and the sines equal to the small angles. Higher order terms, involving the product of sines, vanish. The equation (8) reduces to

$$\underbrace{R_{321}(\theta,\phi,\psi)=R(z,\theta)\,R(y,\phi)\,R(x,\psi)}_{small\theta,\phi,and\psi}=\begin{bmatrix}1 & -\theta & \phi\\ \theta & 1 & -\psi\\ -\phi & \psi & 1\end{bmatrix} \tag{9}$$

Irrespective of the order of matrix multiplication, i.e., for any of the six Euler sequences in which the axes are not repeated, this same form is obtained for small angles of rotation. This is useful because, in practice, we encounter small angular errors associated with linear motions of machine tool carriages in precision machines.

Suppose we want to capture the angular errors associated with the linear motion of a machine carriage which is sliding over a guideway along the x-axis (say). Let frame $\mathfrak{F}_C$ be attached to a point on the carriage whose motion is aligned with the scale. Let frame $\mathfrak{F}_G$ be a global frame attached to the guideway. Replacing the symbols ψ,ϕ, and θ in equation (9) by $\varepsilon_x(x),\varepsilon_y(x)$, and $\varepsilon_z(x)$, respectively, we obtain the following rotation matrix which will represent this rotation due to small angular errors as a function of carriage translation over the guideway along the x-axis

$${}^{\mathfrak{F}_G}R_{\mathfrak{F}_C}=\begin{bmatrix}1 & -\varepsilon_z(x) & \varepsilon_y(x)\\ \varepsilon_z(x) & 1 & -\varepsilon_x(x)\\ -\varepsilon_y(x) & \varepsilon_x(x) & 1\end{bmatrix} \tag{10}$$

where the subscripts on ε represent the axis about which the angular error is reckoned, and we considered all the angular errors to be small. Since small rotations commute, we do not worry about the order in which rotations about each of the three axes were reckoned, as the result is always the same.

8. Modeling general motion

For pure rotation, we found a form for coordinate transformations, namely equation (6), which is convenient for two reasons. First, successive rotation matrices just need to be multiplied. Second, we can go back and forth between frames by premultiplying by the inverses of matrices, which are just the transposes of the respective matrices, thanks to orthogonality of the rotation matrices.

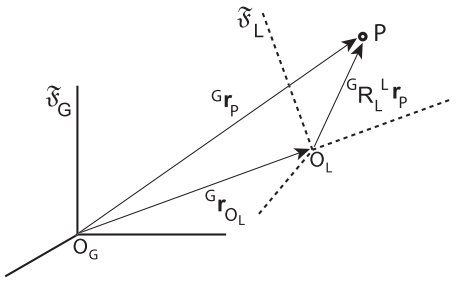

Fig. 7. General motion of a rigid body in a global frame, $\mathfrak{F}_G$. The local frame $\mathfrak{F}_L$ is fixed on to the rigid body.

Can we find such a convenient form for coordinate transformations, when translation of frames is combined with rotation, to model general rigid body motion?

Fig. 7 shows a general motion of a rigid body in a global frame, $\mathfrak{F}_G$. The local frame $\mathfrak{F}_L$ is fixed on to the rigid body. Let $\mathfrak{F}_L$ be originally aligned identically with $\mathfrak{F}_G$ with their origins coinciding. We can decompose the motion of $\mathfrak{F}_L$ as follows {Chasles–Mozzi–Cauchy theorem (Whittaker, 1917; Baruh, 1999)}

(1) A general rotation of the rigid body, $\mathfrak{F}_L$, in a global frame, $\mathfrak{F}_G$, about the origin of $\mathfrak{F}_G$.
(2) A general translation of the origin of the rigid body, $\mathfrak{F}_L$, in the global frame, $\mathfrak{F}_G$.

Based on Fig. 7, vector addition yields

$${}^G\mathbf{r}_P={}^GR_L\,{}^L\mathbf{r}_P+{}^G\mathbf{r}_{O_L} \tag{11}$$

where we have been careful to ensure that all the three vectors are coordinatized in the same reference frame {in this case, $\mathfrak{F}_G$}.

Can we write the right hand side (RHS) of the above equation in the same form as we had in pure rotation? In other words, can we rewrite equation (11) in compact notation as follows

$${}^G\mathbf{r}_P={}^G\mathfrak{T}_L\,{}^L\mathbf{r}_P \tag{12}$$

where ${}^G\mathfrak{T}_L$ is a transformation matrix?

Doing so would give us certain advantages. We could go back and forth from one reference frame to the other merely through matrix inversion. Also, successive motions could be modeled by a simple product of the relevant transformation matrices. We note that we cannot achieve these objectives if the transformations involves vector/matrix addition as in equation (11).

Let us write out equation (11) in expanded form to get a sense of what we are talking about

$$\underbrace{\begin{Bmatrix}{}^Gx_P\\ {}^Gy_P\\ {}^Gz_P\end{Bmatrix}}_{{}^G\mathbf{r}_P}=\underbrace{\begin{pmatrix}r_{11} & r_{12} & r_{13}\\ r_{21} & r_{22} & r_{23}\\ r_{31} & r_{32} & r_{33}\end{pmatrix}}_{{}^GR_L}\underbrace{\begin{Bmatrix}{}^Lx_P\\ {}^Ly_P\\ {}^Lz_P\end{Bmatrix}}_{{}^L\mathbf{r}_P}+\underbrace{\begin{Bmatrix}{}^Gx_{O_L}\\ {}^Gy_{O_L}\\ {}^Gz_{O_L}\end{Bmatrix}}_{{}^G\mathbf{r}_{O_L}} \tag{13}$$

where the leading superscripts in the column vectors refer to the frame in which the components are coordinatized, and the trailing subscripts identify the point whose position that column vector represents.

Similarly, let us write out equation (12) in expanded form to examine its RHS

$$\underbrace{\begin{Bmatrix}{}^Gx_P\\ {}^Gy_P\\ {}^Gz_P\end{Bmatrix}}_{{}^G\mathbf{r}_P}=\underbrace{\begin{pmatrix}t_{11} & t_{12} & t_{13}\\ t_{21} & t_{22} & t_{23}\\ t_{31} & t_{32} & t_{33}\end{pmatrix}}_{{}^G\mathfrak{T}_L}\underbrace{\begin{Bmatrix}{}^Lx_P\\ {}^Ly_P\\ {}^Lz_P\end{Bmatrix}}_{{}^L\mathbf{r}_P} \tag{14}$$

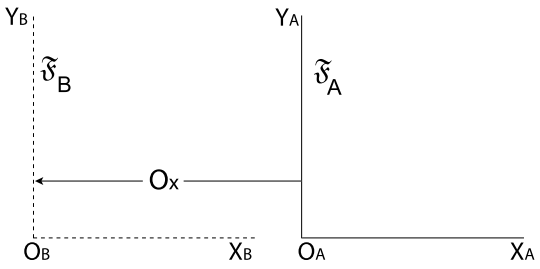

Fig. 8. Linear motion of $\mathfrak{F}_B$ w.r.t. $\mathfrak{F}_A$ along the x-axis by an amount O_x in the negative-x direction.

Clearly, there is no way to write the RHS of equation (13) in the same form as the RHS of equation (14). We must find a way to write ${}^G\mathfrak{T}_L$ differently, because the 3×3 matrix form is not going to work. We accomplish this task by invoking **homogeneous coordinates** (Donmez, 1985; Slocum, 1992), which enable us to express the RHS of equation (13) in compact form.

In a 3-D Cartesian coordinate system, the homogeneous coordinates of the position of a point P(x,y,z) are expressed as (x, y, z, ω), where ω is a scaling factor. For our purpose, we will take the scaling factor as unity. The scaling factor acts as a placeholder, allowing us to use the compact notation. Using homogeneous coordinates, we rewrite equation (13) as follows

$$\underbrace{\begin{Bmatrix} {}^G x_P \\ {}^G y_P \\ {}^G z_P \\ 1 \end{Bmatrix}}_{{}^G\mathbf{r}_P} = \underbrace{\begin{bmatrix} r_{11} & r_{12} & r_{13} & {}^G x_{O_L} \\ r_{12} & r_{22} & r_{23} & {}^G y_{O_L} \\ r_{13} & r_{23} & r_{33} & {}^G z_{O_L} \\ 0 & 0 & 0 & 1 \end{bmatrix}}_{{}^G T_L} \underbrace{\begin{Bmatrix} {}^L x_P \\ {}^L y_P \\ {}^L z_P \\ 1 \end{Bmatrix}}_{{}^L\mathbf{r}_P} \tag{15}$$

where the position vectors are now expressed in homogeneous coordinates, and ${}^G T_L$ is the **homogeneous transformation matrix** (**HTM**) (Donmez, 1985; Slocum, 1992) for transformation of the rigid body configuration from local frame, $\mathfrak{F}_L$, to global frame, $\mathfrak{F}_G$.

The structure of the HTM is to be carefully noted. It is a 4×4 matrix when representing general spatial motion. The top left 3×3 submatrix is just the rotation matrix. The last column is the position vector of the translated origin of the local frame, expressed in homogeneous coordinates. The first three elements of the last row are zero indicating that angles do not warrant scaling.

The coordinates of the translated origin of the local frame, $\mathfrak{F}_L$, with respect to the global frame, $\mathfrak{F}_G$, are also called the **offsets** of $\mathfrak{F}_L$ in $\mathfrak{F}_G$, i.e., the components of ${}^G\mathbf{r}_{O_L}$. While reckoning offsets, we must pay attention to their signs, to correctly reckon the direction of motion.

9. Application to ideal motions

Let us consider the simplest example of ideal translatory motion of frame $\mathfrak{F}_B$ with respect to frame $\mathfrak{F}_A$. The HTM that transforms the coordinates of a point in the frame $\mathfrak{F}_B$, which is offset by an amount O_x in the negative x-direction as shown in Fig. 8, into the reference frame $\mathfrak{F}_A$ is

$${}^A T_B = \begin{bmatrix} 1 & 0 & 0 & -O_x \\ 0 & 1 & 0 & 0 \\ 0 & 0 & 1 & 0 \\ 0 & 0 & 0 & 1 \end{bmatrix} \tag{16}$$

A point to observe is how we took care of the negative x-offset.

Now, let us consider a frame $\mathfrak{F}_B$ rotated by an amount ψ_x in the positive sense about the x-axis of the reference frame $\mathfrak{F}_A$ as shown in Fig. 9. The HTM that transforms the coordinates of a point in the frame

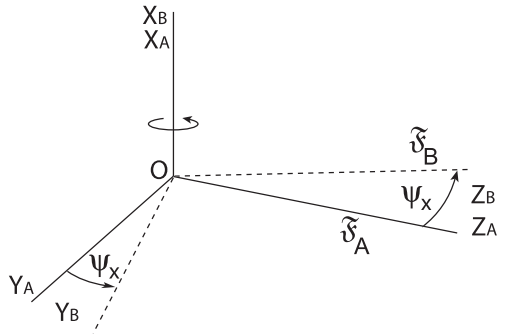

Fig. 9. Rotary motion of $\mathfrak{F}_B$ w.r.t. $\mathfrak{F}_A$ about the x-axis by an amount $+\psi_x$.

$\mathfrak{F}_B$ into the reference frame $\mathfrak{F}_A$ is

$${}^A T_B = \begin{bmatrix} 1 & 0 & 0 & 0 \\ 0 & \cos\psi_x & -\sin\psi_x & 0 \\ 0 & \sin\psi_x & \cos\psi_x & 0 \\ 0 & 0 & 0 & 1 \end{bmatrix} \tag{17}$$

where the submatrix corresponding to rotations is consistent with the rotation matrix $R(x, \psi)$ displayed in equation (7).

Equations (16) and (17) demonstrate the application of the HTM model to ideal motions where no motion errors are considered.

10. Application to machine tool slide motion

We consider machine tools having linear slide motions, i.e. the axes are linear. Doing so keeps the HTMs simpler, because offsets due to linear motions affect only the last column of the HTMs. Rotary axes can also be modeled. Rotary axis offsets affect the rotation submatrix. Though we do not model rotary axes motion in this document, the basic principles that would govern such a model remain the same.

First, we consider a simple motion of a carriage on a slideway. This is a motion along a linear axis (say x). We wish to model the motion of this rigid body (carriage) in a global frame $\mathfrak{F}_G$ attached to the slideway. Let us attach a local frame $\mathfrak{F}_L$ to the carriage. Suppose the carriage moved a distance O_x. If the motion were perfect, all points on the carriage would have traveled this distance O_x along the x-direction. So, the HTM for transformation of coordinates of any point on the rigid body from $\mathfrak{F}_L$ to $\mathfrak{F}_G$ is simply

$${}^G T_L\big|_{\text{nominal}} = \begin{bmatrix} 1 & 0 & 0 & O_x \\ 0 & 1 & 0 & 0 \\ 0 & 0 & 1 & 0 \\ 0 & 0 & 0 & 1 \end{bmatrix} \tag{18}$$

However, the slideway is not perfectly flat or straight. There will be errors associated with the motion. So, the real (imperfect) motion of the carriage can be decomposed into two motions — the above nominal motion, and the error motion. The error motion, associated with a linear move of the carriage in the x-direction, consists of the following components:

(1) The scale error $\delta_x(x)$, also called the linear positioning error of the x-axis (ISO 230-1 2012 E, 2012).
(2) The lateral errors $\delta_y(x)$, and $\delta_z(x)$, also called straightness errors in y and z directions, respectively (ISO 230-1 2012 E, 2012).
(3) The angular errors about the three linear axes $\varepsilon_x(x)$, $\varepsilon_y(x)$, and $\varepsilon_z(x)$, also called the roll, yaw, and pitch errors, respectively (ISO 230-1 2012 E, 2012).

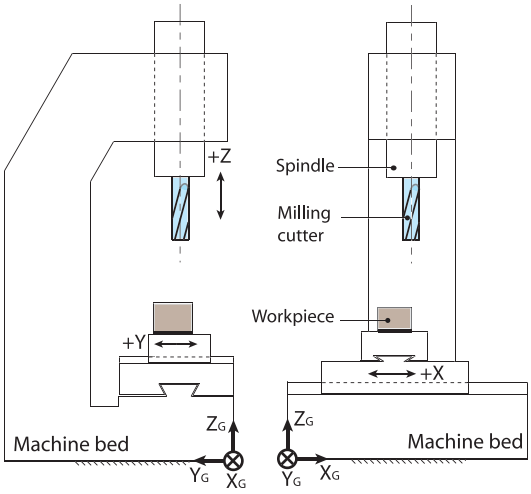

Fig. 10. Schematic sketch of a 3-axis milling machine: front view (right) and left hand side view (left). A global coordinate system $\mathfrak{F}_G(X_G\text{–}Y_G\text{–}Z_G)$ is fixed to the machine bed.

Based on equation (10), the following HTM captures the total error

$$ {}^{G}E_L = \begin{bmatrix} 1 & -\varepsilon_z(x) & \varepsilon_y(x) & \delta_x(x) \\ \varepsilon_z(x) & 1 & -\varepsilon_x(x) & \delta_y(x) \\ -\varepsilon_y(x) & \varepsilon_x(x) & 1 & \delta_z(x) \\ 0 & 0 & 0 & 1 \end{bmatrix} \tag{19} $$

The real (imperfect) motion is, therefore, modeled using the following HTM

$$ {}^{G}T_L\big|_{\text{actual}} = {}^{G}T_L\big|_{\text{nominal}}\ {}^{G}E_L = \begin{bmatrix} 1 & -\varepsilon_z(x) & \varepsilon_y(x) & O_x+\delta_x(x) \\ \varepsilon_z(x) & 1 & -\varepsilon_x(x) & \delta_y(x) \\ -\varepsilon_y(x) & \varepsilon_x(x) & 1 & \delta_z(x) \\ 0 & 0 & 0 & 1 \end{bmatrix} \tag{20} $$

In general, the origin of $\mathfrak{F}_L$ could have three offsets, O_x, O_y, and O_z. Then, the HTM corresponding to axis motion in the x-direction is

$$ {}^{G}T_L\big|_{\text{general}(x)} = \begin{bmatrix} 1 & -\varepsilon_z(x) & \varepsilon_y(x) & O_x+\delta_x(x) \\ \varepsilon_z(x) & 1 & -\varepsilon_x(x) & O_y+\delta_y(x) \\ -\varepsilon_y(x) & \varepsilon_x(x) & 1 & O_z+\delta_z(x) \\ 0 & 0 & 0 & 1 \end{bmatrix} \tag{21} $$

Let us consider a simple machine tool having three linear axes, X-Y-Z. A schematic sketch of such a milling machine is shown in Fig. 10. A global coordinate system $\mathfrak{F}_G$ is fixed to the machine bed.

Now, we consider Fig. 11 which shows the workpiece sitting on the machine bed. Let $\mathfrak{F}_W$ be a local frame fixed to the workpiece. Let $\mathfrak{F}_1$ and $\mathfrak{F}_2$ be frames fixed to the slideways linking the workpiece to the machine bed. The following operation transforms the position vector of a point P coordinatized in $\mathfrak{F}_W$ into the global frame

$$ {}^{G}\mathbf{r}_P = {}^{G}T_2\,{}^{2}T_1\,{}^{1}T_W\,{}^{W}\mathbf{r}_P \tag{22} $$

where the HTMs include the errors and have the general form shown in equation (21).

Similarly, in Fig. 12, let $\mathfrak{F}_T$ be a local frame fixed to the tool and $\mathfrak{F}_S$ be a frame fixed to the spindle linking the tool to the machine bed. The following operation transforms the position vector of a point Q coordinatized in $\mathfrak{F}_T$ into the global system

$$ {}^{G}\mathbf{r}_Q = {}^{G}T_S\,{}^{S}T_T\,{}^{T}\mathbf{r}_Q \tag{23} $$

where the HTMs include the errors and have the general form shown in equation (21).

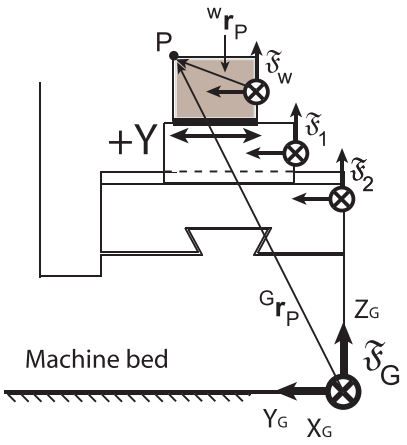

Fig. 11. Sequence of coordinate systems for expressing the position vector of point P on the workpiece in the global coordinate system $\mathfrak{F}_G$.

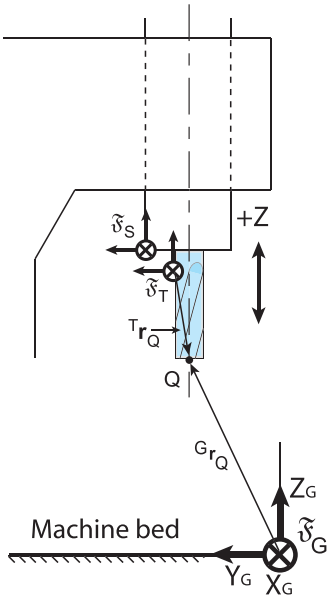

Fig. 12. Sequence of coordinate systems for expressing the position vector of point Q on the tool in the global system $\mathfrak{F}_G$.

Positioning the tool point Q to be at the workpiece point P with accuracy is the same as setting

$$ {}^{G}\mathbf{r}_Q = {}^{G}\mathbf{r}_P \tag{24} $$

From equations (22) and (23), we note that the RHS of the equations will, in general, not be equal. So, in general, the above equation will not hold. So, we make the following nominal correction

$$ {}^{G}\mathbf{r}_{\text{correction}} = {}^{G}\mathbf{r}_Q - {}^{G}\mathbf{r}_P \tag{25} $$

This ${}^{G}\mathbf{r}_{\text{correction}}$ yields the nominal motions the X, Y, and Z axes must make in order to compensate for tool point location errors. This additional motion correction must be provided to the tool point to bring it to the desired location with respect to the workpiece. Alternatively, the workpiece may be appropriately moved in relation to the toolpoint.

11. Student exercise No. 1: Lateral error and Abbé error calculations

The purpose of this exercise is to visualize and quantify the components of error associated with linear motion.

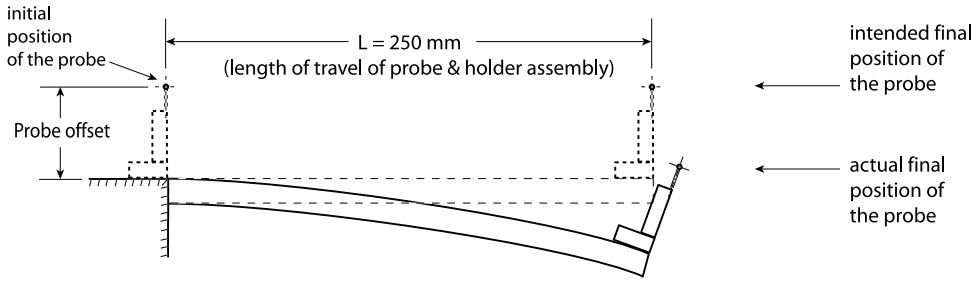

Fig. 13. Position error of a probe due to bending of a cantilever beam under the weight of the probe.

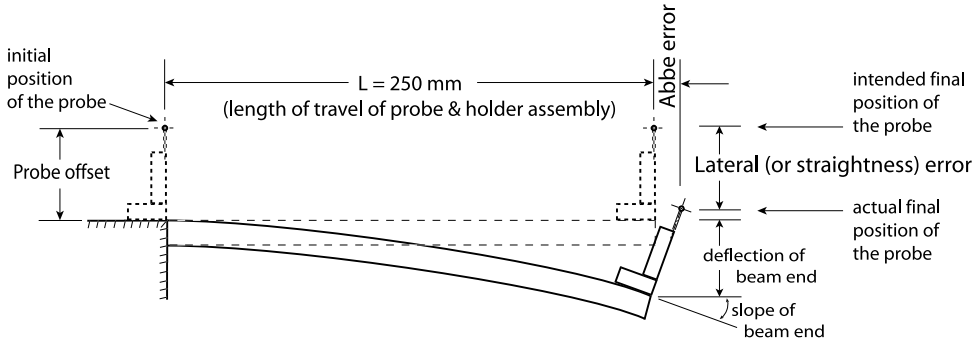

Fig. 14. Identification of lateral (straightness) error and the Abbé offset error.

Fig. 13 shows a probe which has to be moved from its initial position to an intended final position as shown. The probe travels over a cantilever beam ($L = 250$ mm) to a final destination as shown. The cantilever beam has a rectangular cross section (width, $b = 25$ mm and depth, $h = 50$ mm). The weight of the probe and holder assembly is 100 N, which acts perpendicular to the width of the beam. The elastic modulus of the beam is $E = 210$ GPa. The probe offset is $O_z = 100$ mm. The bending of the beam under the weight of the probe introduces error in the final position of the probe. To keep the problem tractable, we ignore the deflection of the beam under its own weight.

Task 1: The student is required to understand the error in the measured final position of the probe, which has two mutually perpendicular components, as opposed to its intended ideal final position in the case where there is no bending of the cantilever beam under the weight of the probe. The student is required to identify these two components by name and label them on the sketch.

The solution to Task 1: The two components are the lateral (straightness) error and the Abbé offset error. These are shown in Fig. 14, which the student is expected to reproduce.

Task 2: The student is required to estimate the two components of the error quantitatively. This is accomplished using elementary elasticity theory.

The solution to Task 2: Under the weight of the probe, the deflection and slope of the end of the cantilever are calculated when the probe has reached its final destination. The area moment of inertia, I, of the cross section of the beam, the vertical deflection of the end of the beam under the weight of the probe, δ, and slope of the end of the beam under weight of the probe, θ, may be found using the following expressions (Timoshenko, 2004)

$$I = \frac{bh^3}{12}, \qquad \delta = \frac{PL^3}{3EI}, \qquad \theta = \frac{PL^2}{2EI} \tag{26}$$

Calculations yield

$\delta = 9.54 \times 10^{-6}$ m $\simeq 10$ μm = the **lateral error**

$\theta \simeq 5.7 \times 10^{-5}$ radian $\simeq 12$ arcsec

$\therefore$ the **Abbé error** = Offset$\times\theta = 0.1$ m$\times 5.7 \times 10^{-5} = 5.7 \times 10^{-6}$ m $\simeq 6$ μm

12. Student exercise No. 2: An HTM for a machine tool slideway

The purpose of this exercise is to develop the ability to specify rotational and linear errors as functions of the motion direction. Additionally, using the offsets of the origin of a coordinate system attached to a machine slideway, in a given reference frame, to develop the ability of assembling the relevant HTM.

The task: For the two axis positioning system shown in Fig. 15, the student is required to symbolically determine the HTM for transforming from coordinate frame 2 (attached to the vertical z-axis) to coordinate frame 1 (attached to the horizontal y axis). The HTM should include the effects of the relevant axis error motions. The y and z offsets between the coordinate frames at the 'home' positions of each axis are provided. There are no offsets between the coordinate frames in the x direction.

The solution: The only possible motion of the frame 2, with respect to frame 1, is in the z direction. Hence, all the δ and ϵ are functions of z alone. The offsets of the origin of frame 2 in frame 1 are as follows

$$^1\mathrm{X}_{\mathrm{offset},2} = 0, \qquad ^1\mathrm{Y}_{\mathrm{offset},2} = +a, \qquad ^1\mathrm{Z}_{\mathrm{offset},2} = +b \tag{27}$$

$\therefore$ the required HTM is

$$^1\mathrm{T}_2 = \begin{bmatrix} 1 & -\varepsilon_z(z) & \varepsilon_y(z) & ^1X_{offset,2} + \delta_x(z) \\ \varepsilon_z(z) & 1 & -\varepsilon_x(z) & ^1Y_{offset,2} + \delta_y(z) \\ -\varepsilon_y(z) & \varepsilon_x(z) & 1 & ^1Z_{offset,2} + \delta_z(z) \\ 0 & 0 & 0 & 1 \end{bmatrix} \tag{28}$$

Substituting the offset values into the above expression we have the desired result

$$^1\mathrm{T}_2 = \begin{bmatrix} 1 & -\varepsilon_z(z) & \varepsilon_y(z) & \delta_x(z) \\ \varepsilon_z(z) & 1 & -\varepsilon_x(z) & a + \delta_y(z) \\ -\varepsilon_y(z) & \varepsilon_x(z) & 1 & b + \delta_z(z) \\ 0 & 0 & 0 & 1 \end{bmatrix} \tag{29}$$

This exercise serves to show why the error elements of the HTM are functions of the linear move of the slide in a specified direction.

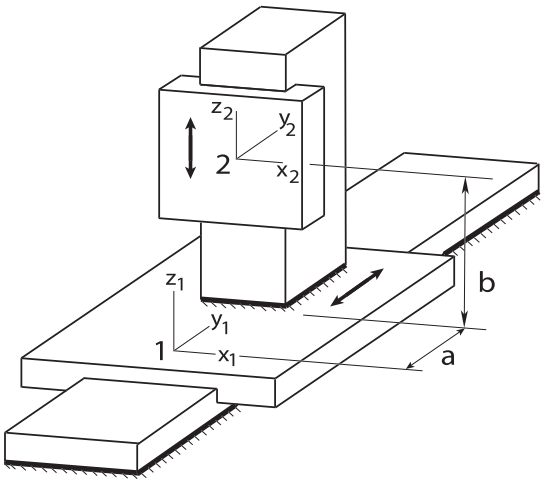

Fig. 15. A two-axis positioning system.

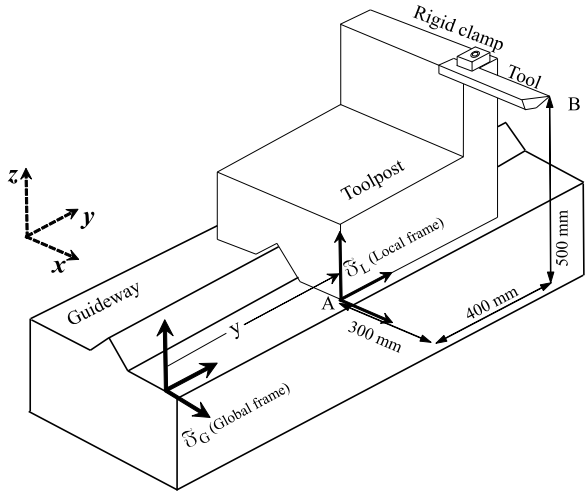

Fig. 16. A prismatic axis oriented along the y-direction. The $x-y-z$ offsets of the toolpoint located at B with respect to the origin of the local frame located at A are +300 mm, +400 mm, and +500 mm, respectively. The local frame is fixed to the toolpost, and the global frame is fixed to the guideway.

Naturally, the HTM itself is a function of the linear move in this direction of slideway motion. The student also learns how to reckon the offsets of the origin of one frame in the other to assemble the entire HTM.

13. Student exercise No. 3: Error calculation over a grid of points

The purpose of this exercise is to develop the ability to calculate the position error of a tool point as a function of slideway motion, given the knowledge of errors associated with the motion of the origin of the reference frame to which the tool is attached.

The task: Fig. 16 shows a nominally single degree-of-freedom prismatic axis oriented in the y-direction, on which a tool is mounted. The position errors have been measured at point A (the origin of the local frame affixed to the tool post). These measured errors are listed in Table 1. The student is required to find $\delta_y(y)$ as they would appear at the tool point (located at B) which is offset from the origin of the local frame. The x–y–z-offsets of the tool point B from the origin of the local frame are $a = +300$ mm, $b = +400$ mm and $c = +500$ mm, respectively.

The solution: What is essentially stated is that the toolpost moves along the y-direction in a ground (global) frame, and the origin of the local axis fixed to this toolpost has an erroneous motion with reference to the commanded y-axis motion. These errors are measured and listed in Table 1 as a function of the position of the toolpost along the y-axis in the global frame. Using this data, the student needs to find the position of the tool point in the global frame as a function of the y-axis advance of the tool post. The tool point is offset with respect to the origin in the local frame. The difference between the actual and nominal y-coordinate value of the tool point in the global frame is the position error of the tool point. The y-component of this error is $\delta_y(y)\Big|_B$, which is to be calculated. The y-component of the nominal position is merely $b + y$.

Let the position vector of the toolpoint in homogeneous coordinates be ${}^L\mathbf{r}_B$ in the local frame and ${}^G\mathbf{r}_B$ in the global frame. These are related as follows

$$ {}^G\mathbf{r}_B = {}^G\mathbf{T}_L \; {}^L\mathbf{r}_B \tag{30} $$

where ${}^G\mathbf{T}_L$ is the relevant HTM transforming from local to global homogeneous coordinates, and ${}^L\mathbf{r}_B$ is specified in the problem statement as

$$ {}^L\mathbf{r}_B = \begin{bmatrix} a & b & c & 1 \end{bmatrix}^T = \begin{bmatrix} 300\text{ mm} & 400\text{ mm} & 500\text{ mm} & 1 \end{bmatrix}^T \tag{31} $$

As the toolpost advances, for any value of y, the HTM can be populated based on the error data listed in Table 1 using interpolation. Since the commanded motion is along the y-axis, all the elements of the HTM will be functions of y alone. The form of the HTM which captures the error, will be analogous to equation (19).

With no loss of generality, for convenience, we choose the ground frame, G, to coincide with the local frame, L, at the beginning of the motion so that

$$ {}^G\mathrm{X}_{\mathrm{offset},L} = 0, \qquad {}^G\mathrm{Y}_{\mathrm{offset},L} = 0, \qquad {}^G\mathrm{Z}_{\mathrm{offset},L} = 0 \tag{32} $$

This results in the following expression for ${}^G\mathbf{r}_B$ based on the equations (30), (31) and (32)

$$ \begin{Bmatrix} {}^G x_B \\ {}^G y_B \\ {}^G z_B \\ 1 \end{Bmatrix} = \begin{bmatrix} 1 & -\varepsilon_z(y) & \varepsilon_y(y) & \cancelto{0}{{}^G\mathrm{X}_{\mathrm{offset},L}} + \delta_x(y) \\ \varepsilon_z(y) & 1 & -\varepsilon_x(y) & \cancelto{0}{{}^G\mathrm{Y}_{\mathrm{offset},L}} + \delta_y(y) \\ -\varepsilon_y(y) & \varepsilon_x(y) & 1 & \cancelto{0}{{}^G\mathrm{Z}_{\mathrm{offset},L}} + \delta_z(y) \\ 0 & 0 & 0 & 1 \end{bmatrix} \begin{Bmatrix} a \\ b+y \\ c \\ 1 \end{Bmatrix} \tag{33} $$

In this problem, we are merely interested in finding the numerical value of ${}^G y_B$, which is the element in the second row. So, we need not perform the entire matrix multiplication. We merely write out the required expression corresponding to the second row as

$$ \begin{aligned} {}^G y_B &= (b+y) + \delta_y(y)\Big|_B = a\,\varepsilon_z(y) + (b+y) - c\,\varepsilon_x(y) + \delta_y(y) \\ \Rightarrow \delta_y(y)\Big|_B &= a\,\varepsilon_z(y) - c\,\varepsilon_x(y) + \delta_y(y) \end{aligned} \tag{34} $$

This solves the problem. Substituting from Table 1, we may obtain the numerical values for $\delta_y(y)\Big|_B$ from $y = 0$ to 8 mm.

It is worth noting that the above expression for $\delta_y(y)\Big|_B$ could have been written down by arguing from first principles. The x-offset rotated about the z-axis by an amount equal to the z-axis rotational error yields a linear error contribution in the y-direction. Similarly, the z-offset rotated about the x-axis yields a linear error contribution in the y-direction. The y-offset does not yield any contribution as it is fixed. The linear y-component error of the origin of the local frame contributes the last term. Of course, in reality, we are interested in all the three components of the linear error, and we need to write everything in a compact manner in matrix algebra form for computational ease. So, we use the HTM formulation.

Using equation (34) the values of $\delta_y(y)\Big|_B$ are calculated and listed in the Table 2. The student can note that the effects of tool offsets

Table 1
Data for student exercise No. 3: Measured position errors of the origin of the local frame in the global frame as a function of the commanded y-axis motion referenced in the global frame.

y (commanded) (mm)	$\delta_x(y)$ (μm)	$\delta_y(y)$ (μm)	$\delta_z(y)$ (μm)	$\varepsilon_x(y)$ (arc-sec)	$\varepsilon_y(y)$ (arc-sec)	$\varepsilon_z(y)$ (arc-sec)
0	0	0	0	0	0	0
1	0.4	−0.3	0.2	- 7	7	- 6
2	1.0	−0.6	0.6	- 16	19	15
3	2.2	−0.2	0.5	- 18	24	26
4	3.6	0.2	−0.1	- 20	23	19
5	1.2	0.9	−0.4	7	17	23
6	−0.6	1.4	−0.5	14	- 6	10
7	−0.9	0.8	−0.3	19	- 17	- 1
8	−0.4	0.5	0	17	- 23	- 9

Table 2
Solution to student exercise No. 3: Calculated tool point position errors $\delta_y(y)\big|_B$.

Commanded ${}^G y_A$ (mm):	0	1	2	3	4	5	6	7	8
Measured $\delta_y(y)\big\|_A$ (μm):	0	−0.3	−0.6	−0.2	0.2	0.9	1.4	0.8	0.5
Calculated $\delta_y(y)\big\|_B$ (μm):	0	8	60	81	76	17	−18	−47	−54

can be very large even with very small position errors (linear and rotational). The results of this problem show that small position errors in the motion of the slideway can get highly amplified at the tool point. This numerical result also reveals the futility of manufacturing super accurate machines. Even though the linear position errors of the slideway motion were of submicron magnitude, and the rotational errors were of arc-second magnitude, the linear errors at the tool point were highly magnified by an order of magnitude. So, error compensation is unavoidable for accurate machining. Hence the importance of the HTM model.

At this point students sometime ask why we could not measure the toolpoint location errors directly just as we measured the location errors of the slide. This question hits at the core of the Bryan principle. The answer is that we cannot place scales wherever the toolpoint moves. We are restricted to place the measuring scales at some fixed locations on the slideway.

14. Discussion

The purpose of the HTM model is to transform locally referenced motion errors into the tool-workpiece position error, or the probe-workpiece position error, depending on whether it is a tool or a probe. It is very hard to measure the relative position of the tool/probe point with respect to the workpiece. In general, no accurate tools exists to achieve this objective. So, in a serial linked machine, we move one axis at a time, keeping the others fixed, measure the 6-degrees-of-freedom errors associated with each such axis motion, and use the information in the HTM model to obtain an equivalent error between the tool and the workpiece.

Well developed standards exist for characterizing the geometric accuracy of machines (ISO 230-1 2012 E, 2012), repeatability of positioning of axes (ISO 230-2 2014 E, 2014), and accuracy of axes of rotation (ISO 230-7 2015 E, 2015). A technical report documenting the characteristics of precision measuring instruments for testing the geometric accuracy of machine tools, operating either under no-load or under quasi-static conditions, also exists (ISO/TR 230-11 2018 E, 2018).

While moving along an axis in one direction, the errors turn out to be a little different compared with moving in the reversed direction. This owes to backlash resulting in so called ‘lost motion,’ or ‘reversal error,’ or ‘hysteresis.’ Donmez et al. (1986) mention that “though hysteresis is actually a systematic error, it is separated out for convenience because it is repeatable, its sign depends on direction of travel along the axis, and that it may be compensated for if the approach direction is known and an adequate pre-travel is made”.

At this point, a remark on machine accuracy is in order. We turn to Slocum (1992) to get a quantitative sense of machine accuracy, which is as follows: The structural loop is the path that the load takes from the tool to the workpiece. If the characteristic component accuracy (which may be reckoned in parts per million) is multiplied by the length of the structural loop, an indication of machine accuracy (part per million) may be obtained.

In modern CNC machine tools and CNC coordinate measuring machines, **linear error compensation** is widely employed (Donmez et al., 1986; Slocum, 1992). There is only so much accuracy that can be built into a machine by construction. The marginal return on investment in increased costs, to manufacture highly accurate structures, is not justified. Moreover, stiffness of any structure is never infinite. So, we do not bother to construct super-accurate machine tool structures. Instead, we focus on stability, repeatability and correction of inaccuracies by compensation in software. The HTM model, first proposed by Donmez (1985), lies at the heart of this strategy.

Though we have discussed the geometric accuracy of machine tools used to produce machined parts, exactly the same strategy of error compensation is applied in coordinate measuring machines (Zhang et al., 1985). Indeed, in coordinate measuring applications, the effect of the operational inaccuracies are comparatively small. Two major sources of operational inaccuracies are absent, i.e., there are no deformations due to cutting forces, and there are no tool wear effects. Of course, there are thermal effects, and clamping accuracy effects.

Is it worthwhile to study geometric accuracies when compared with operational inaccuracies? Owing to the bewildering variety, sizes, and precision levels of machine tools, it is hardly possible to generalize as to what fraction of the errors are due to which factor. Yet, the question must be answered. It suffices to address the issue by limiting the discussion to high precision machines.

Slocum (1992) has remarked on the design strategy for high precision machines using error budgets. An error budget is a low cost tool which helps evaluate design concepts before spending time and money on performing analysis such as solid modeling and finite elements. Errors may be broken down into four types: geometric, load induced, thermal, and process errors, the last three of which constitute what has been termed operational errors in this article. Slocum (1992) mentions that for high precision machines, if there is a balanced allocation of resources at the machine design stage, the magnitude of each of these error components will be equal.

Once the machine has been built, it no longer behooves us to pose the question of the relative magnitudes of inaccuracies due to different types of error as a matter of post-mortem. The issue has to be addressed and settled at the design stage to ensure a "balanced design" such that the four components of error are of approximately equal magnitude. According to Slocum (1992) the geometric-based error budget must be developed to be four times better than required using HTM based spreadsheets, which lets the designer create the overall geometry and spacing of elements. Subsequently, solid models and finite elements are used to make sure that thermal and load-induced deflections are within limits.

Upon assembly of the physical machine, the post-mortem, specific to each individual machine, and for a given process, can certainly be done. As an illustrative example, we may consider Schmitz et al. (2008) who compared the relative importance of error sources for a milling process using a general purpose CNC milling machine. Error sources studied included quasi-static geometric, thermal induced geometric, spindle thermal growth, contouring, and surface location errors due to stable forced vibrations in cutting. The effects of the first three sources on part dimensions was studied using an HTM approach integrated into a Monte Carlo simulation. The cutting force induced error was found to dominate, but it was reported that this component could become insignificant at slightly different cutting speeds. The machine effectively compensated for spindle thermal growth. Thermal growth of the machine contributed an additional and equal effect to the cold state geometric error.

For pedagogical purposes, comments on learning outcomes are warranted. Here, we share the intended outcomes that have been relevant to us while teaching this topic. Other teachers may well have a different set of outcomes, though we expect a significant amount of overlap. The intended outcomes may differ owing to differences in programs, program outcomes, student preparedness, and time constraints, among other things. Our intended student learning outcomes have been the following: after studying this module, students should be able to

(1) Identify the two broad factors affecting machined part accuracy, i.e., geometrical and operational inaccuracies (thermal, dynamic, and process related).
(2) Describe the sources of machine tool accuracy, i.e., constructional, and measuring scale location based, as captured by the Abbé principle.
(3) Recognize the fact that the effects of geometrical accuracies can be overcome by compensation is software.
(4) Demonstrate how to mathematically capture motion based errors using the HTM model.
(5) Apply the HTM model to compensate for erroneous toolpoint location with respect to the workpiece to reduce machined part inaccuracies, and to perform elementary calculations to this effect.
(6) Recognize the fact that this method of compensation in software is indispensable in coordinate measuring machines where dynamic errors are negligible, and thermal errors are actively controlled, making geometric inaccuracies play a dominant role in affecting measurement accuracies.

15. Concluding remarks

The method of presenting the subject evolved out of the experience of teaching undergraduate classes at the University of Florida and Mahindra University. Though Tlusty (Tlusty, 1999) has provided an excellent discussion of machining accuracy, the HTM model is neither developed explicitly in his text, nor is the method applied to tool-workpiece positioning error in the way we have done here. These two aspects, deriving the HTM model from first principles in a compact manner, and its application to a 3-axis machine tool as an illustrative example, comprise our unique contributions to the presentation of the subject to undergraduate students. We hope that this topic will eventually find its way into standard textbooks on manufacturing, and that the method presented here will be taught. We share our experiences in this article, and we hope that fellow teachers will have an opportunity to use it in their teaching efforts. All the necessary information is laid out here in fair detail.

Declaration of competing interest

The authors declare that they have no known competing financial interests or personal relationships that could have appeared to influence the work reported in this paper.

References

Abbé, E., 1890. Messapparate für Physiker. Zeitschrift Für Instrumentenkunde 10.
Baruh, H., 1999. Analytical Dynamics. WCB/McGraw Hill, Singapore.
Black, J.T., Kohser, R.A., 2019. DeGarmo's Materials and Processes in Manufacturing, 13th ed. John Wiley & Sons, Inc., Hoboken, NJ.
Bryan, J.B., 1979. The Abbé principle revisited: An updated interpretation. Precis. Eng. 1 (3).
Donmez, M.A., 1985. A general methodology for machine tool accuracy enhancement: Theory, application and implementation. (Ph.D. thesis). Purdue University, West Lafayette, IN.
Donmez, M.A., Blomquist, D.S., Hocken, R.J., Liu, C.R., Barash, M.M., 1986. A general methodology for machine tool accuracy enhancement by error compensation. Precis. Eng. 8 (4).
Ghosh, A., Mallik, A.K., 1992. Manufacturing Science, second ed. Affiliated East-West Press Pvt. Ltd., New Delhi, India.
Groover, M.P., 2013. Fundamentals of Modern Manufacturing, fifth ed. John Wiley & Sons, Inc., Hoboken, NJ.
Hogben, L., 2007. Handbook of Linear Algebra. Chapman & Hall/CRC, Boca Raton, FL.
ISO 230-1:2012 E, 2012. Test code for machine tools part 1: Geometric accuracy of machines operating under no-load or quasi-static conditions. Standard, International Organization for Standardization, Geneva, CH.
ISO 230-2 2014 E, 2014. Test code for machine tools part 2: Determination of accuracy and repeatability of positioning of numerically controlled axes. Standard, International Organization for Standardization, Geneva, CH.
ISO 230-7 2015 E, 2015. Test code for machine tools part 7: Geometric accuracy of axes of rotation. Standard, International Organization for Standardization, Geneva, CH.
ISO/TR 230-11 2018 E, 2018. Test code for machine tools part 11: Measuring instruments suitable for machine tool geometry tests. Standard, International Organization for Standardization, Geneva, CH.
Kalpakjian, S., Schmid, S.R., 2018. Manufacturing Engineering and Technology, seventh ed. Pearson Education, Inc., New York, NY.
Leach, R., 2014. The international academy for production engineering. In: Laperrière, L., Reinhart, G. (Eds.), In: CIRP Encyclopedia of Production Engineering, Springer, Berlin, Heidelberg, Germany.
Schey, J.A., 2012. Introduction to Manufacturing Processes, third ed. McGraw Hill Education.
Schmitz, T.L., Ziegert, J.C., Canning, J.S., Zapata, R., 2008. Case study: A comparison of error sources in high-speed milling. Precis. Eng. 32.
Schuster, M.D., 1993. A survey of attitude representations. J. Astonaut. Sci. 41 (4).
Slocum, A.H., 1992. Precision Machine Design. Prentice-Hall, Englewood Cliffs, NJ.
Timoshenko, S., 2004. Strength of Materials Part 1: Elementary Theory and Problems, third ed. CBS Publishers & Distributors, New Delhi.
Tlusty, J., 1999. Manufacturing Processes and Equipment. Prentice Hall, Upper Saddle River, NJ.
Whittaker, E.T., 1917. A Treatise on the Analytical Dynamics of Particles and Rigid Bodies, second ed. Cambridge University Press, London, UK.
Zhang, G., Veale, R., Borchardt, B., Hocken, R., 1985. Error compensation of coordinate measuring machines. Ann. CIRP 34 (1).